HHS Public Access

Author manuscript

Nat Chem Biol. Author manuscript; available in PMC 2015 March 01.

Published in final edited form as:

Nat Chem Biol. 2014 September ; 10(9): 707–709. doi:10.1038/nchembio.1589.

Endosomal GPCR signaling turned off by negative feedback actions of PKA and v-ATPase

Alexandre Gidon[1], **Mohammad M. Al-Bataineh**[2], **Frederic G. Jean-Alphonse**[1], **Hilary Stevenson**[3], **Tomoyuki Watanabe**[4], **Claire Louet**[1], **Ashok Khatri**[4], **Guillermo Calero**[3], **Núria M. Pastor-Soler**[2], **Thomas J. Gardella**[4], and **Jean-Pierre Vilardaga**[1,*]

[1]Laboratory for GPCR Biology, Department of Pharmacology & Chemical Biology, University of Pittsburgh, School of Medicine, Pittsburgh, PA 15261, USA

[2]Renal-Electrolyte Division, University of Pittsburgh, School of Medicine, Pittsburgh, PA 15261, USA

[3]Department of Structural Biology Department of Medicine, University of Pittsburgh, School of Medicine, Pittsburgh, PA 15261, USA

[4]Endocrine Unit, Massachusetts General Hospital and Harvard Medical School, Boston, MA 0114, USA

Abstract

The PTH receptor is one of the first GPCR found to sustain cAMP signaling after internalization of the ligand–receptor complex in endosomes. This unexpected model is adding a new dimension on how we think about GPCR signaling, but its mechanism is incompletely understood. We report here that endosomal acidification mediated by the PKA action on the v-ATPase provides a negative feedback mechanism by which endosomal receptor signaling is turned-off.

The parathyroid hormone (PTH) receptor (PTHR) is a medically important G-protein coupled receptor (GPCR) that triggers critical signaling processes in bone and kidney cells to regulate Ca^{2+} homeostasis. We recently discovered that PTH or its recombinant N-terminal fragment PTH(1–34) sustains G-protein activity and cAMP production after PTHR internalization into early endosomes by an emergent model of GPCR signaling, where β-arrestins promote and retromer attenuates cAMP signaling[1–3]. This model has been validated for another GPCR[4], but the cellular events responsible for shifting signaling receptor–arrestin complexes to receptor–retromer complexes that do not signal remain

*To whom correspondence should be addressed: jpv@pitt.edu.

Competing financial interests

The authors declare no competing financial interests.

Author contributions

A.L.G. performed most of the experiments with support of C.L. and F.G.J-A. H.S. and G.C performed thermostability assays. T.D. and T.J.G. conducted all of the radioligand binding experiments. M.M.A-B. and N.M.P-S. conducted phosphorylation assays. A.K. synthesized all peptides. All authors contributed to discussions. J-P.V., A.L.G. and T.J.G. analyzed the data. J-P.V and A.L.G. designed the project. J.P.V. supervised the overall study, and wrote the manuscript with support of A.L.G.

unknown. Here we show that sustained cAMP mediated by the internalized PTH–PTHR complex is turned off by endosomal acidification as a consequence of a negative feedback mechanism involving PKA and the vacuolar proton pump v-ATPase.

Our previous finding that sustained cAMP signaling induced by PTH(1–34) (hereafter noted PTH) is derived from internalized PTH–PTHR complexes residing in intracellular compartments labeled by Rab-5 suggest a key role of early endosomes in this process[2]. We confirmed this observation by using a dominant negative mutant of Rab5, Rab5-S34N, which prevents the internalization of plasma membrane associated receptor and the formation of early endosomes[5]. HEK-293 cells stably expressing the PTHR and this mutant were no able to generate a sustained cAMP response mediated by PTH, thus indicating that prolonged PTHR signaling takes place in Rab5-positive endosomes (Fig. 1a).

We next observed that the duration of cAMP mediated by PTH correlated well with the time course required for the endosomal Rab5-to-Rab7 conversion (Fig. 1b), a process dependent on endosomal acidification and that triggers the maturation of early endosomes into late endosomes[6]. Cells expressing either Rab5 or Rab7 labeled with GFP ($Rab5^{GFP}$ or $Rab7^{GFP}$, respectively) were challenged with PTH^{TMR}, a fully functional PTH(1–34) labeled with tetramethylrhodhamine[7] (Supplementary Results, Supplementary Fig. 1). A quantitative analysis of colocalization using Pearson's correlation coefficient revealed that a few minutes after ligand challenge, PTH^{TMR} localized mainly in Rab5-labeled endosomes. At later time points when the extent of cAMP decreased (Fig. 1a, control), the presence of PTH^{TMR} on Rab5-labelled endosomes decreased while increasing on Rab7 endosomes (Fig. 1b). We reasoned that pH changes encountered in endosomes during the Rab5-Rab7 shift might be a key determinant for the duration of PTHR signaling in early endosomes.

We tested this hypothesis by examining the effect of endosomal pH on PTHR signaling and ligand binding. To this end, we treated cells with a specific inhibitor of the activity of the v-ATPase, bafilomycin-A_1, known to block endosomal acidification and late-stage vesicle maturation[8]. To ascertain that bafilomycin prevented endosomal acidification, we estimated the pH of endosomes by recording the emission of internalized PTH(1–34) tagged with FITC (PTH^{FITC}), a fluorophore with a strict linear dependence in fluorescence emission over the pH range 4.0 to 8.0 as opposed to PTH^{TMR} (Supplementary Fig. 2). Cells expressing the PTHR C-terminally tagged with CFP ($PTHR^{CFP}$) that were challenged with PTH^{FITC} showed an initial pH value of 7.2 corresponding to the extracellular pH (Fig. 1c). A few minutes later pH values declined concomitantly to the internalization of PTH–PTHR complexes in early endosomes, as indicated by the colocalization between PTH^{TMR} and either $Rab5^{GFP}$ (Supplementary Fig. 1) or $PTHR^{GFP}$, a PTHR N-terminally tagged with GFP (Supplementary Fig. 3a). The addition of bafilomycin fully blocked endosomal acidification (Fig. 1c) without affecting PTHR internalization (Supplementary Fig. 3b), thus confirming the efficacy of the approach.

In the following series of experiments we recorded FRET between $PTHR^{GFP}$ and PTH^{TMR} as a readout for ligand–receptor interactions[7]. We observed that the dissociation began $\approx$ 15 min after removal of the ligand (Fig. 1d), a time point when the endosomal pH reached a value of 6.5 (Fig. 1c). Cells treated with bafilomycin remarkably prolonged the association

between PTH^{TMR} and $PTHR^{GFP}$ (Fig. 1d) at times when the ligand/PTHR complex is localized in early endosomes as indicated by the colocalization between PTH^{TMR} and either $Rab5^{GFP}$ (Fig. 1b) or $PTHR^{GFP}$ (Supplementary Fig. 3b).

The effect of pH on the rates of dissociation of PTH that we observed in endosomes was mimicked *in vitro* by using radioligand assays. We thus examined in cell membrane extracts the effect of pH on the rates of dissociation of complexes formed between the PTHR and the [^{125}I]-radiolabeled version of PTH(1–34). The rate and extent of dissociation of [^{125}I]-PTH(1–34) increased progressively as the pH decreased from 7.2 to 4.1, and occurred quite significantly at pH values encountered in early endosomes (pH < 6.5) (Fig. 1e). Together, these data show that the dissociation between PTHR and PTH is pH dependent and takes place in acidified endosomes with a pH < 6.5.

We questioned whether acidic pH values found in endosomes cause unfolding of the PTHR structure as a mean to weaken the interaction with PTH. We addressed this question by determining the pH dependence of the PTHR thermostability by using purified PTHR[9]. We found that the melting temperature (T_m°C) of PTHR significantly increased when pH values decreased from 8.5 to 7.0, but remained constant at acidic pH detected in early endosomes (Fig. 1f) indicating that the PTHR structure is more rigid at endosomal pH. The binding of PTH had no significant effect on PTHR thermostability implying that the fastest release of PTH at endosomal pH can therefore be attributed to a decrease in ligand–receptor affinity rather that a change in PTHR conformation or thermal damage on PTHR.

As we have obtained evidence that PTH dissociated from PTHR at pH values encountered in early endosomes, we hypothesized that pH sensitivity in the PTH–PTHR association regulates the duration of PTHR signaling in early endosomes. We tested this hypothesis by determining the consequences of endosomal pH changes for the magnitude and duration of PTH-mediated cAMP production. Using an intramolecular FRET biosensor[10] to monitor cAMP in live cells, we found that treatment of HEK-293 cells stably expressing PTHR with bafilomycin alone had no effect on cAMP production (Supplementary Fig. 4a), but markedly prolonged cAMP signaling by PTH (Fig. 1a). Bafilomycin had no effect on duration of signaling mediated by the β-adrenergic receptor agonist isoproterenol, but extended the duration of the vasopressin V2 receptor signaling in response to vasopressin (AVP), which is another GPCR system that continues to signal after internalization[4] (Supplementary Fig. 4a). Similar results were obtained by using an alternative method to measure cAMP in cells (Supplementary Fig. 4b). The effect of bafilomycin on PTH signaling was further confirmed in osteoblastic-like ROS17/2.8 cells expressing endogenously the PTHR (Fig. 2a, b). Consistent with earlier studies[11] done with this cells, cAMP production triggered by PTH persisted after an initial decline, and bafilomycin significantly increased the prolonged cAMP induced by challenge with PTH. Taken together, these results suggest that signaling by PTH is terminated by the acidification of the endosomal lumenal compartment.

We recently showed that the generation of cAMP mediated by internalized PTH–bound PTHR is promoted by the interaction of PTHR with β-arrestins and is attenuated by the interaction with the retromer complex in endosomes[3]. What event shifts signaling PTHR–

arrestin complexes to inactive PTHR–retromer complexes? We sought to answer this question by comparing the influence of endosomal pH on the duration of PTHR–arrestin and PTHR–retromer complexes. For this, we recorded FRET between PTHR tagged with CFP ($PTHR^{CFP}$) and either β-arrestin 2 (βarr2) or the retromer subunit Vps35 each tagged with YFP ($\beta arr2^{YFP}$ or $Vps35^{YFP}$, respectively) in endosomes. We found that dissociation of $PTHR^{CFP}$–$\beta arr2^{YFP}$ complexes coincided with the formation of $PTHR^{CFP}$–$Vps35^{YFP}$ complexes (Supplementary Fig. 5a). The absence of endosomal acidification by bafilomycin caused a persistent association between β-arr2 and PTHR in response to PTH, a situation that both prevented PTHR interaction with retromer (Supplementary Fig. 5b) and that fully counteracted the capacity of retromer to inhibit cAMP (Supplementary Fig. 5c). This indicates that shifting signaling PTHR–βarr complexes to inactive PTHR–retromer complexes is a direct consequence of endosomal acidification rather than β-arrestins and retromer competing for PTHR binding.

We next sought to determine whether PTHR signaling regulates its own deactivation process by promoting endosomal acidification. Given that activity of the v-ATPase is positively regulated by PKA phosphorylation[12], we tested this hypothesis by using a PKA phosphorylation deficient v-ATPase variant that displays a lower catalytic activity[12]. We first determined the capacity of PTH to phosphorylate the v-ATPase. We found that PTH induced a significant phosphorylation of the wild type v-ATPase tagged with the Flag epitope ($v\text{-}ATPase^{Flag}$), but not in cells treated with H89 (Supplementary Fig. 6d) or expressing its PKA phosphorylation-deficient variant (Fig. 2c) indicating that the v-ATPase is a phosphorylation target for the PTH/PTHR/PKA system. The finding that PTH did not phosphorylate the v-ATPase mutant led us predict that its activity was decreased. We tested this prediction by measuring the change in pH during PTH–PTHR internalization. We found that changes in endosomal pH were dampened by overexpression of the PKA phosporylation-deficient v-ATPase mutant (Fig. 2d), prolonging the duration of cAMP production mediated by PTH (Fig. 2e). Consistent with the effects observed with the v-ATPase mutant and further supporting the involvement of PKA in the regulation of endosomal PTHR signaling, inhibition of PTH-mediated PKA activity by H89 (Supplementary Fig. 6a) blocked endosomal acidification (Fig. 2d) without preventing PTHR internalization or PTHR–βarr2 association (Supplementary Fig. 6b, c), and kept PTHR signaling in HEK-293 (Fig. 2e) or ROS17/2.8 cells (Fig. 2a, b). Taken together, these results indicate that PKA activity is required to reduce endosomal pH via the v-ATPase, thus providing an efficient negative feedback loop to terminate PTHR signaling at the endosomes.

Consistent with the role of PKA activation in endosomal acidification, cholera toxin (CTX), which catalyses the ADP-ribosylation on $G\alpha_S$ causing a persistent activation of the Gs/cAMP/PKA system, has been found in complex with the ADP-ribosylation factor (ARF6) and $G\alpha_S$ in endosomes while increasing endosomal H^+ transport[13]. In keeping with endosomal acidification, influential studies in the 70–80's characterizing the endocytic pathway of cell surface receptors for diverse ligands[14–18,19,20,21] showed that the acidification of early endosomes is a key causative event that initiates ligand–receptor dissociation permitting receptors to recycle to the cell surface[22]. The importance of acidified

endosomes for GPCR recycling and resensitization has been later reported for the β_2-adrenergic receptor[23].

In addition to explain that endosomal acidification is responsible for PTH–PTHR dissociation, our findings summarized in the model presented in Fig. 2f imply that sustained cAMP levels originated from internalized PTH–PTHR complexes are regulated by a negative feedback mechanism where PTH-mediated PKA activation leads to v-ATPase phosphorylation and subsequent endosomal acidification, which in turn results in the disassembly of signaling PTH–PTHR–arrestin complexes and assembly of inactive PTHR–retromer complexes. This mechanism extends the paradigm in the regulation of endosomal GPCR signaling where they can turn themselves off by a negative-feedback loop involving PKA and the v-ATPase.

Online Methods

Cell culture and transfection

Cell culture reagents were obtained from Invitrogen (Carlsbad, CA). Human embryonic kidney cells (HEK-293) (ATCC, Georgetown, DC) were cultured in DMEM supplemented with 10% fetal bovine serum at 37°C in a humidified atmosphere containing 5% CO_2. HEK-293 cells stably expressing the recombinant human PTHR were grown in selection medium (DMEM, 10 % FCS, penicillin/streptomycin 5%, 500 μg/ml neomycin). Culturing of rat osteosarcoma (ROS17/2.8) cells was done as described[11]. For transient expression, cells cultured in 6-well plates were transfected with the appropriate cDNAs using Fugene-6 (Roche) when they reached 70% confluency, usually 24 to 48 h before experiments. Cells were then plated on poly-D-Lysine coated coverslips 24 h after transfection. We have optimized expression conditions to ensure the expression of fluorescent-labeled proteins was similar in examined cells by performing experiments in cells displaying comparable fluorescence levels.

Laser Scanning Confocal Microscopy

Cells plated on coverslips were mounted in Attofluor cell chambers (Life Technologies) and incubated with Hepes buffer containing 150 mM NaCl, 10 mM Hepes, 2.5 mM KCl and 0.2 mM $CaCl_2$, 0.1% BSA, pH 7.4 were transferred on the Nikon Ti-E microscope (Nikon) equipped with a Z-driven piezo motor. Imaging were acquired using Nikon A1 confocal unit, through a 60X N.A=1.45 objective (Nikon). CFP, GFP or FITC, YFP, Tomato and mCherry were excited with 440, 488, 514 and 560 nm lasers (Melles Griot), respectively. Emission fluorescences were acquired using a Spectral Detection mode and collected by a 32-channels PMT. Typically, a Z-stack of 4 to 8 images (Z step = 500 nm) was acquired every 5 minutes during 45 to 60 minutes. Data acquisitions were done using Nikon Element Software (Nikon Corporation). After acquisition, raw data were spectrally deconvoluted using Nikon Element Software (Nikon). Every different analysis was done at the single cell level.

Confocal Data Analysis

For colocalization analysis, region of interest were drawn around cells based on maximum intensity projection, and colocalization was calculated for each time point using Pearson's correlation algorithm from Nikon Element Software. For FRET analysis, region of interest were drawn around cells based on maximum intensity projection. For every time point, the total amount of fluorescence for each plane were collected, summed and subtracted from the background. Ratio between YFP and CFP or mCherry/dTomato and GFP were then calculated and corrected as described[24].

pH measurements

First, we determined the relationship between FITC fluorescence and pH. To this end, 100 nM of PTH(1–34) labeled with FITC (PTH^{FITC}) was added to buffer solution with different pH values (from 7.2 to 4). For each pH conditions, images were acquired with the same acquisition parameters as used for the experiment. FITC level of fluorescence were extracted, normalized to the value obtained for pH 7.2 and plotted over pH value. Second, HEK293 cells plated on coated glasses were transfected with PTHR C-terminally tagged with CFP (PTHR-CFP), mounted in Attofluo cell chambers (Life Technologies) and incubated with HEPES buffer. Cells were challenged by 100 nM PTH^{FITC} for < 1 minute. Fluorescence emissions were recorded as described above. Data obtained after spectral deconvolution were analyzed as follow: a) region of interests were drawn around each single cells; b) respective FITC and CFP fluorescence levels (F_{FITC} and F_{CFP}, respectively) were recorded; c) the ratio F_{FITC}/F_{CFP} were plotted overtime. Note that CFP emission permits to normalize the variation of FITC due to variation in total amount and focus changes; d) the ratio F_{FITC}/F_{CFP} was normalized by t = 1 value; e) pH was estimated by comparison with the linear relationship between FITC fluorescence and pH determined using 100 nM PTH^{FITC} in buffers at diverse pH values.

Drugs treatment

For inhibition of PKA or v-ATPase activity, cells plated on coverslips were pre-incubated with 2 μM H89 or 20 nM Bafilomycin A1 (Sigma Aldrich) diluted in HEPES buffer, for 15 minutes at 37°C. Cells were continuously perfused with HEPES buffer (containing H89 or bafilomycin) or with 100 nM PTH for the time indicated in horizontal bars (less than 1 minute). For v-ATPase inhibition, after addition of 100 nM PTH for 1 minute, cells were washed with FRET buffer containing H89 or Bafilomycin A1.

Radioligand dissociation

Plasma membrane extracts and radioligand were preincubated for 90 min to allow ligand–receptor complex formation. The dissociation phase was then initiated by the addition of an excess of the unlabeled analog of the radioligand (100 nM final concentration). Immediately before this addition (t = 0), and at successive time points thereafter, 200 μl aliquots (corresponding to 30,000 cpm) were withdrawn and immediately processed by vacuum filtration, as previously described[25]. Nonspecific binding was determined in parallel reaction tubes containing the unlabeled analog (100 nM) in both the preincubation and dissociation

phases. The specifically bound radioactivity at each time point was calculated as a percent of the radioactivity specifically bound at t = 0.

Thermostability

Thermal denaturation assays were adapted from the work of Alexandrov and colleagues[26]. N-[4-(7diethylamino-4methyl-3 coumarinyl)phenyl]maleimide (CPM) and sample mixtures were protected from light at all stages to prevent photobleaching. CPM dye powder (Sigma) was dissolved in DMSO (Sigma) at a concentration of 4 mg/ml, aliquoted and stored at −80°C. Stock solution was diluted 1:40 in DMSO immediately before used. Reactions were performed in sextuplicate with a total reaction volume of 20 μl. Purified PTHR was prepared as previously reported[9] (Supplementary Fig. 9). 10 μg of purified PTHR were used for each reaction in a buffer (100 mM NaCl, 150 mM Tris-HCl) with varying pH from 5.0 to 8.5 with or without 10 μM PTH(1–34) (Bachem) with the addition of 6 μl of diluted CPM dye for each replicate. PTHR-CPM reaction mixtures were prepared in MicroAmp Fast Optical 96-Well Reaction Plates (Applied Biosystems). Thermal melt curves were performed using a StepOnePlus (Applied Biosystems) using the protein melt curve program with a 25–95°C, 1% gradient. A custom dye calibration was performed to use CPM as a reporter. Melt curve data was processed in the Protein Thermal Shift Software (Applied Biosystems).

Measurements of cAMP and PKA activity

Cyclic AMP was assessed using either FRET-based assays[24,27] or a bioluminescent assay with the Glosensor cAMP reporter (Promega Corp.)[28,29], and PKA activity was measured by FRET-based assays[30]. For FRET measurements, cells were transiently transfected with FRET based biosensors for either cAMP (epac1-CFP/YFP) or PKA activity (AKARIII-CFP/YFP), and measurements were performed and analyzed as previously described[24,27]. FRET signals were monitored after challenge with either PTH(1–34) or PTH analogs (both 100 nM). In brief, HEK293 cells plated on poly-D-lysine coated glass were mounted in Attofluor cell chambers (Life Technologies), maintained in Hepes buffer and transferred on the Nikon Ti-E equipped with an oil immersion 40X N.A 1.30 Plan Apo objective and a moving stage (Nikon Corporation). CFP and YFP were excited using a mercury lamp. Fluorescence emissions were filtered using a 480 ± 20 nm (CFP) and 535 ± 15 nm (YFP) filter set and collected simultaneously with a LUCAS EMCCD camera (Andor Technology) using a DualView 2 (Photometrics) with a beam splitter dichroic long pass of 505 nm. Fluorescence data were extract form single cell using Nikon Element Software (Nikon Corporation). The FRET ratio for single cells was calculated and corrected as previously described[24]. Note that the maximal cAMP response corresponds to 90% of a cAMP response mediated by forskolin. Individual cells were continuously perfused with buffer or with the ligand (100 nM) for the time indicated by the horizontal bar.

For cAMP measurements by bioluminescence we used HEK- 293-derived cell lines that stably express the Glosensor cAMP reporter[28,29]. Cells in 96-well plates were pre-loaded with 0.5 mM luciferin for 30 min, treated with buffer or 20 nM Bafilomycin-A1 for 15 min, and then with the indicated ligand for 15 min. Cells were washed twice after ligand treatment, and then fresh buffer containing luciferin was added (t = 0), and cAMP-dependent luminescence was recorded for 3 h in a PerkinElmer Plate PE Envision reader.

Phosphorylation assay in cells

HEK-293 cells expressing the PTH receptor were transiently transfected to express either wild-type (WT-A) or Ser-175 to Ala (S175A-A) mutant Vacuolar H^+-ATPase (V-ATPase) A subunit[12]. Two days after transfection, cells were treated with PTH (100 nM) or vehicle control (water) for 10 min. After this treatment the cells were harvested in ice-cold lysis buffer using our established techniques[12,31]. Protein concentration was then determined for each of the lysed samples. The WT-A and S175A-A subunits were immunoprecipitated from 500 μg of each of the pre-cleared lysates using the M2 anti-FLAG monoclonal antibody (Sigma-Aldrich, St. Louis, MO, USA) coupled to protein A/G beads (Pierce Biotechnology, Rockford, lL, USA). Immunoprecipitation in the absence of the anti-FLAG antibody was also performed as a control. After three washes in lysis buffer, the immunoprecipitation samples were eluted in sample buffer and subjected to SDS-PAGE (4–12% gradient gel; Nu-PAGE, Life Technologies, Grand Island, NY, USA). After transfer onto nitrocellulose membranes, immunoblotting was performed with either: 1) A phospho-(Ser/Thr) PKA Substrate Antibody (1:5,000 dilution, raised in rabbit, Cell Signaling Technology, Danvers, MA, USA), followed by the appropriate secondary antibody coupled to HRP as needed (GE Healthcare Biosciences, Pittsburgh, PA, USA) or 2) the anti-FLAG antibody coupled to HRP (1:100,000 dilution, raised in mouse, Sigma). The probed protein was then visualized and quantified using a VersaDoc Imager with Quantity One software (Bio-Rad, Hercules, CA, USA). The PKA-phosphorylated substrate signal relative to the control condition was quantified and normalized to FLAG blot signal re-probed on the same blot.

Statistical Analysis

Data are expressed as mean values ± s.e.m. Statistical analyses were performed using the unpaired Student's t-test when applicable. Differences were considered significant at $P < 0.05$.

Supplementary Material

Refer to Web version on PubMed Central for supplementary material.

Acknowledgments

This work was supported by the National Institute of Diabetes and Digestive and kidney Diseases (NIDKK) of the National Institutes of Health (NIH) under Award numbers R01 DK087688 (to J-P.V.), P01 DK11794 (project I to T.J.G.), R01 DK08184 (to N.M.P.-S.), F32 DK097889 (to M.M.A-B.), and the Cellular Physiology Core of the P30 DK079307 "Pittsburgh Kidney Research Center". The authors thank Dr. Kenneth R. Hallows for his suggestions on the v-ATPase phosphorylation assay.

References

1. Vilardaga JP, Gardella TJ, Wehbi VL, Feinstein TN. Non-canonical signaling of the PTH receptor. Trends Pharmacol Sci. 2012; 33:423–31. [PubMed: 22709554]
2. Ferrandon S, et al. Sustained cyclic AMP production by parathyroid hormone receptor endocytosis. Nat Chem Biol. 2009; 5:734–42. [PubMed: 19701185]
3. Feinstein TN, et al. Retromer terminates the generation of cAMP by internalized PTH receptors. Nat Chem Biol. 2011; 7:278–84. [PubMed: 21445058]
4. Feinstein TN, et al. Noncanonical control of vasopressin receptor type 2 signaling by retromer and arrestin. J Biol Chem. 2013; 288:27849–60. [PubMed: 23935101]

5. Stenmark H, et al. Inhibition of rab5 GTPase activity stimulates membrane fusion in endocytosis. EMBO J. 1994; 13:1287–96. [PubMed: 8137813]
6. Clague MJ, Urbe S, Aniento F, Gruenberg J. Vacuolar ATPase activity is required for endosomal carrier vesicle formation. J Biol Chem. 1994; 269:21–4. [PubMed: 8276796]
7. Castro M, Nikolaev VO, Palm D, Lohse MJ, Vilardaga JP. Turn-on switch in parathyroid hormone receptor by a two-step parathyroid hormone binding mechanism. Proc Natl Acad Sci U S A. 2005; 102:16084–9. [PubMed: 16236727]
8. van Weert AW, Dunn KW, Geuze HJ, Maxfield FR, Stoorvogel W. Transport from late endosomes to lysosomes, but not sorting of integral membrane proteins in endosomes, depends on the vacuolar proton pump. J Cell Biol. 1995; 130:821–34. [PubMed: 7642700]
9. Pullara F, et al. A general path for large-scale solubilization of cellular proteins: from membrane receptors to multiprotein complexes. Protein Expr Purif. 2013; 87:111–9. [PubMed: 23137940]
10. Nikolaev VO, Bunemann M, Hein L, Hannawacker A, Lohse MJ. Novel single chain cAMP sensors for receptor-induced signal propagation. J Biol Chem. 2004; 279:37215–8. [PubMed: 15231839]
11. Wehbi VL, et al. Noncanonical GPCR signaling arising from a PTH receptor-arrestin-Gbetagamma complex. Proc Natl Acad Sci U S A. 2013; 110:1530–5. [PubMed: 23297229]
12. Alzamora R, et al. PKA regulates vacuolar H+-ATPase localization and activity via direct phosphorylation of the a subunit in kidney cells. J Biol Chem. 2010; 285:24676–85. [PubMed: 20525692]
13. El Hage T, Merlen C, Fabrega S, Authier F. Role of receptor-mediated endocytosis, endosomal acidification and cathepsin D in cholera toxin cytotoxicity. FEBS J. 2007; 274:2614–29. [PubMed: 17451437]
14. Basu SK, Goldstein JL, Anderson RG, Brown MS. Monensin interrupts the recycling of low density lipoprotein receptors in human fibroblasts. Cell. 1981; 24:493–502. [PubMed: 6263497]
15. Brown MS, Goldstein JL. Receptor-mediated endocytosis: insights from the lipoprotein receptor system. Proc Natl Acad Sci U S A. 1979; 76:3330–7. [PubMed: 226968]
16. Goldstein JL, Brown MS, Anderson RG, Russell DW, Schneider WJ. Receptor-mediated endocytosis: concepts emerging from the LDL receptor system. Annu Rev Cell Biol. 1985; 1:1–39. [PubMed: 2881559]
17. Brown MS, Goldstein JL. Regulation of the activity of the low density lipoprotein receptor in human fibroblasts. Cell. 1975; 6:307–16. [PubMed: 212203]
18. Borden LA, Einstein R, Gabel CA, Maxfield FR. Acidification-dependent dissociation of endocytosed insulin precedes that of endocytosed proteins bearing the mannose 6-phosphate recognition marker. J Biol Chem. 1990; 265:8497–504. [PubMed: 2160460]
19. Rao K, van Renswoude J, Kempf C, Klausner RD. Separation of Fe+3 from transferrin in endocytosis. Role of the acidic endosome. FEBS Lett. 1983; 160:213–6. [PubMed: 6576912]
20. Harford J, Bridges K, Ashwell G, Klausner RD. Intracellular dissociation of receptor-bound asialoglycoproteins in cultured hepatocytes. A pH-mediated nonlysosomal event. J Biol Chem. 1983; 258:3191–7. [PubMed: 6298227]
21. Harford J, Wolkoff AW, Ashwell G, Klausner RD. Monensin inhibits intracellular dissociation of asialoglycoproteins from their receptor. J Cell Biol. 1983; 96:1824–8. [PubMed: 6304116]
22. Hsu VW, Bai M, Li J. Getting active: protein sorting in endocytic recycling. Nat Rev Mol Cell Biol. 2012; 13:323–8. [PubMed: 22498832]
23. Krueger KM, Daaka Y, Pitcher JA, Lefkowitz RJ. The role of sequestration in G protein-coupled receptor resensitization. Regulation of beta2-adrenergic receptor dephosphorylation by vesicular acidification. J Biol Chem. 1997; 272:5–8. [PubMed: 8995214]
24. Vilardaga JP, Romero G, Feinstein TN, Wehbi VL. Kinetics and dynamics in the G protein-coupled receptor signaling cascade. Methods Enzymol. 2013; 522:337–63. [PubMed: 23374192]
25. Dean T, Vilardaga JP, Potts JT Jr, Gardella TJ. Altered selectivity of parathyroid hormone (PTH) and PTH-related protein (PTHrP) for distinct conformations of the PTH/PTHrP receptor. Mol Endocrinol. 2008; 22:156–66. [PubMed: 17872377]
26. Alexandrov AI, Mileni M, Chien EY, Hanson MA, Stevens RC. Microscale fluorescent thermal stability assay for membrane proteins. Structure. 2008; 16:351–9. [PubMed: 18334210]

27. Vilardaga JP. Studying ligand efficacy at G protein-coupled receptors using FRET. Methods Mol Biol. 2011; 756:133–48. [PubMed: 21870223]

28. Binkowski BF, Fan F, Wood KV. Luminescent biosensors for real-time monitoring of intracellular cAMP. Methods Mol Biol. 2011; 756:263–71. [PubMed: 21870231]

29. Binkowski BF, et al. A luminescent biosensor with increased dynamic range for intracellular cAMP. ACS Chem Biol. 2011; 6:1193–7. [PubMed: 21932825]

30. Sample V, et al. Regulation of nuclear PKA revealed by spatiotemporal manipulation of cyclic AMP. Nat Chem Biol. 2012; 8:375–82. [PubMed: 22366721]

31. Alzamora R, et al. AMP-activated protein kinase regulates the vacuolar H+-ATPase via direct phosphorylation of the A subunit (ATP6V1A) in the kidney. Am J Physiol Renal Physiol. 2013; 305:F943–F956. [PubMed: 23863464]

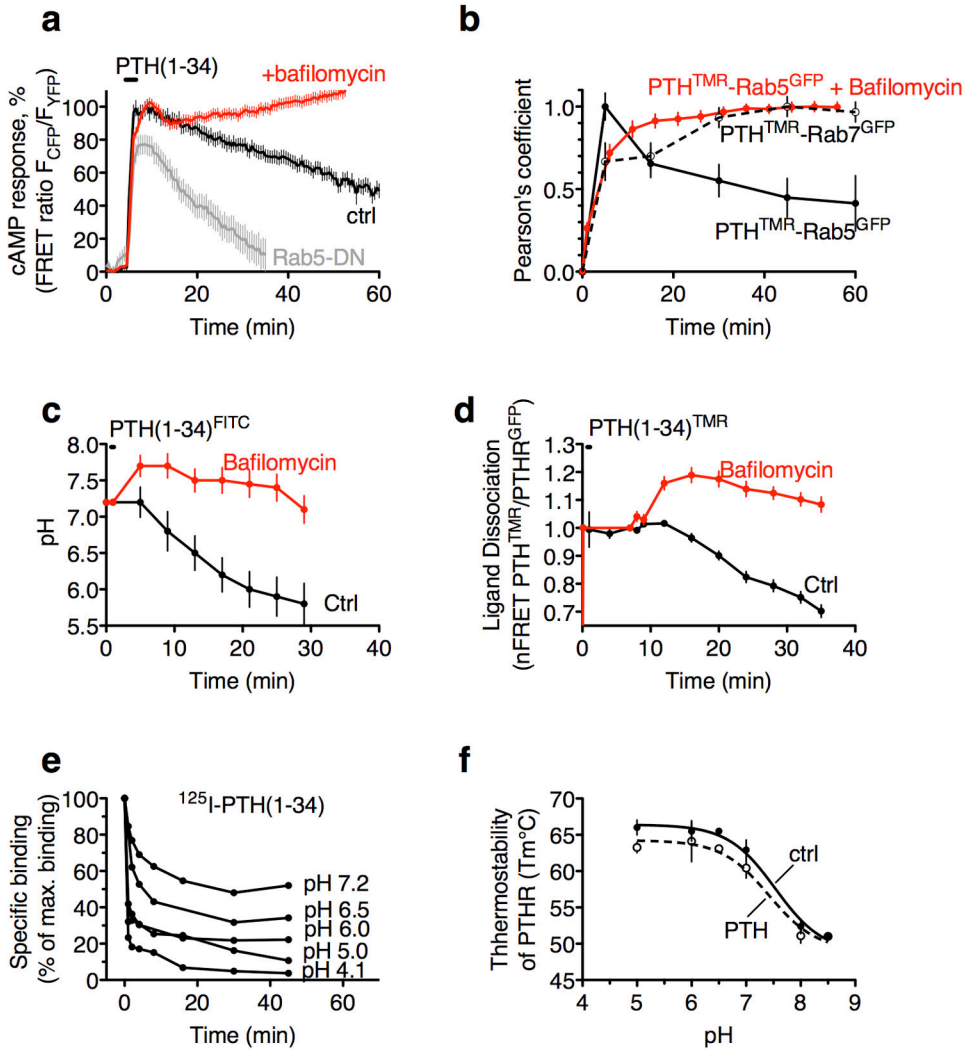

Figure 1. Effect of endosomal pH on PTHR signaling

(**a**) Averaged time-courses of cAMP production in response to PTH in HEK293 cells stably expressing the PTHR and the cAMP biosensor, epac-CFP/YFP. Individual cells were continuously perfused with buffer or with the ligand (100 nM) for the time indicated by the horizontal bar. Data represent mean values ± s.e.m. of five independent experiments and *n* = 80 cells for each condition. (**b**) Colocalization of PTH(1–34)^{TMR} and the early endosome marker, Rab5^{GFP}. Cells were briefly perfused (20 s) with 100 nM of PTH(1–34)^{TMR} and then with buffer alone for the remainder of the experiment. Data represent mean values ± s.e.m. of three independent experiments and *n* = 32 cells. (**c**) Recording pH using PTH^{FITC} in HEK293 cells expressing PTHR C-terminally tagged with CFP. Estimates were made using FITC fluorescence data together with the pH standard plot showed in Supplementary Fig. 2a. Data represent mean values ± s.e.m. of five independent experiments and *n* = 46 (control) and *n* = 71 (bafilomycin) cells. (**d**) Averaged dissociation time-courses of PTH(1–34)^{TMR} from PTHR N-terminally labeled with GFP. FRET recordings from HEK-293 cells treated with or without bafilomycin are shown as normalized ratio. Data represent mean values ± s.e.m. of three independent experiments and *n* = 68 (control) and *n* = 71

(bafilomycin) cells. (**e**) Time course of ^{125}I-PTH(1–34) dissociation at varying pH (n = 3). (**f**) Thermostability of the PTHR alone or associated with PTH(1–34) at varying pH (n = 3).

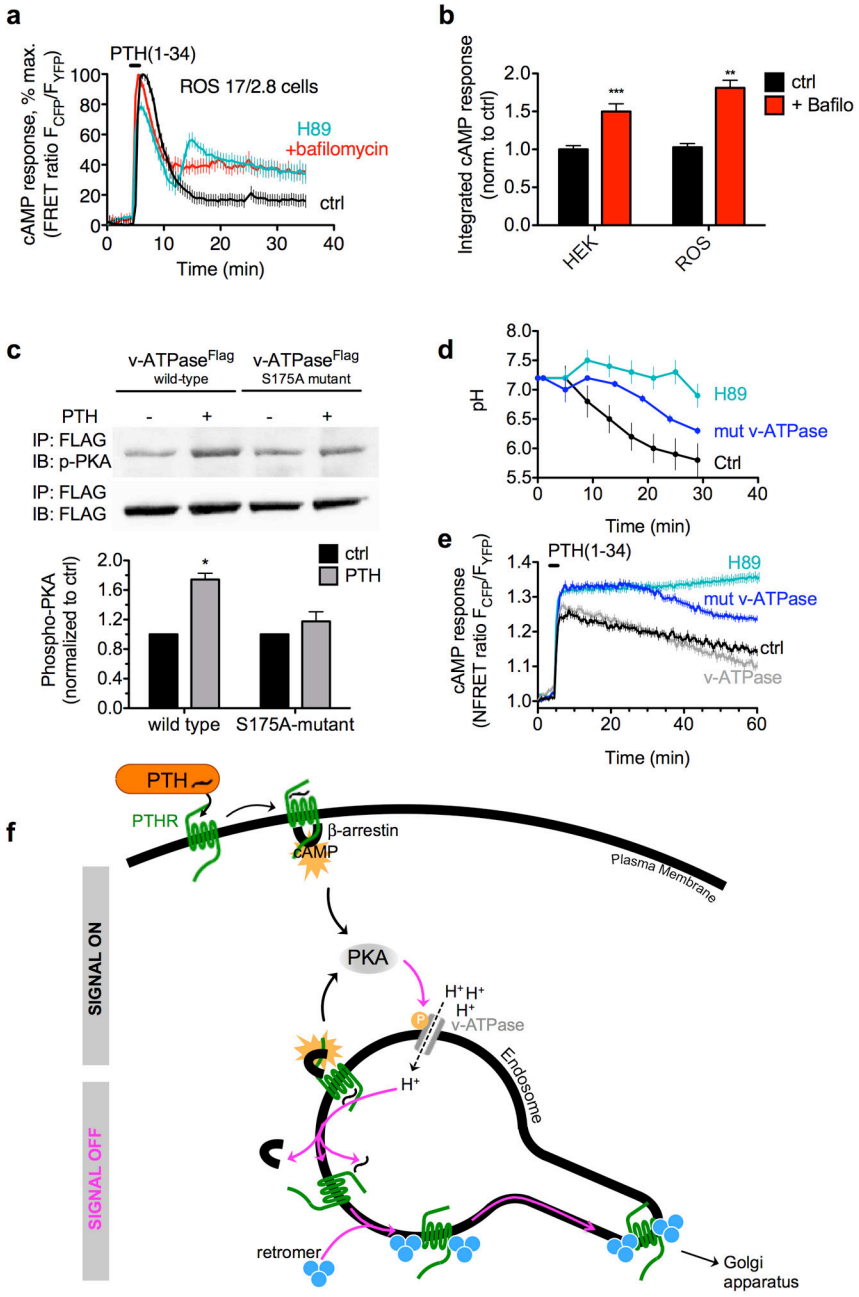

Figure 2. Negative feedback mechanism

(**a**) Cyclic AMP responses in osteosarcoma cells. Similar cAMP measurements as described in Fig. 1a were performed on ROS18/2.8 cells. Data represent the mean ± sem of 4 independent experiments and n = 50 (ctrl), n = 50 (bafilomycin), and n = 50 (PKA) cells. (**b**) Bars compare the averaged cAMP responses in ROS 17/2.8 (panel d) and HEK-293 cells (Fig. 1a) that is determined by measuring the area under the curve from 0 to 30 min of experiments. (**f**) Proposed model for shutting down PTHR signaling. A new regulatory mechanism of PTHR signaling where sustained cAMP signaling after receptor internalization is turned off by a negative feedback mechanism involving PKA and the v-

ATPase. **(c)** Representative set of immunoblot of an immunoprecipitation experiment using the PKA phosphorylation substrate-specific antibody (*upper*) and FLAG (*lower*). Bars represent the mean ± s.e.m of $n = 5$ ($^{*}P < 0.05$). (**d**) Recording pH using PTH^{FITC} as described in Fig. 1c. Data represent the mean ± s.e.m. of five independent experiments and $n = 45$ (control), $n = 50$ (mut v-ATPase) and n = 57 (H89) cells. (**e**) Averaged time-courses of cAMP production in response to 100 nM PTH in live HEK293 cells stably expressing the PTHR as described in Fig. 1a. Data represent mean values ± s.e.m. of five independent experiments and $n = 40$ (control), $n = 79$ (H89), $n = 124$ (v-ATPase), and $n = 173$ (mut v-ATPase) cells.